

Supporting Information

Mechanical rigidity of a shape-memory metal-organic framework increases by crystal downsizing

Al A. Tiba, Matthew T. Conway, Collin S. Hill, Dale C. Swenson, Leonard R. MacGillivray, and Alexei V. Tivanski**

Department of Chemistry, University of Iowa, Iowa City, IA, 52242-1294 USA.

*Corresponding authors: len-macgillivray@uiowa.edu; alexei-tivanski@uiowa.edu

- 1) Synthesis of micro- and nanodimensional $[\text{Cu}_2(\text{bdc})_2(\text{bpy})]_n$ crystals
- 2) Powder X-ray diffraction (PXRD) measurements
- 3) Atomic Force Microscopy (AFM) imaging and nanoindentation measurements
- 4) References

1) Synthesis of micro- and nanodimensional $[\text{Cu}_2(\text{bdc})_2(\text{bpy})]_n$ crystals (bdc = 1,4-benzenedicarboxylate, bpy = 4,4'-bipyridine)

Materials: Copper (II) sulfate pentahydrate, terephthalic acid, and 4,4'-bipyridine were purchased from Sigma Aldrich and used without further purification.

Micro-sized crystals of $[\text{Cu}_2(\text{bdc})_2(\text{bpy})]_n$ were grown *via* solvothermal reaction. Copper (II) sulfate pentahydrate (0.103 g), terephthalic acid (0.07 g), and bpy (0.033 g) were ground using a mortar-and-pestle and added to a MeOH (66 mL) solution containing 0.5 mL formic acid. The mixture was placed into a Teflon-lined steel autoclave at 120 °C for 3 days. A blue-green precipitate was collected, washed with MeOH, and dried overnight at 75 °C. The product was comprised of plate-like crystals with sizes ranging from 50 nm to 20 μm , as revealed by AFM imaging and optical microscopy (Fig. 1). Nano-sized crystals were grown *via* an established coordination modulation method.¹

2) Powder X-ray diffraction (PXRD) measurements

PXRD data were obtained on a Bruker D500 X-ray diffractometer using Cu $K\alpha_1$ radiation ($\lambda = 1.54056 \text{ \AA}$) (scan type: locked coupled; scan mode: continuous; step size: 0.02° ; scan time: 2s/step). The samples were mounted on glass slides.

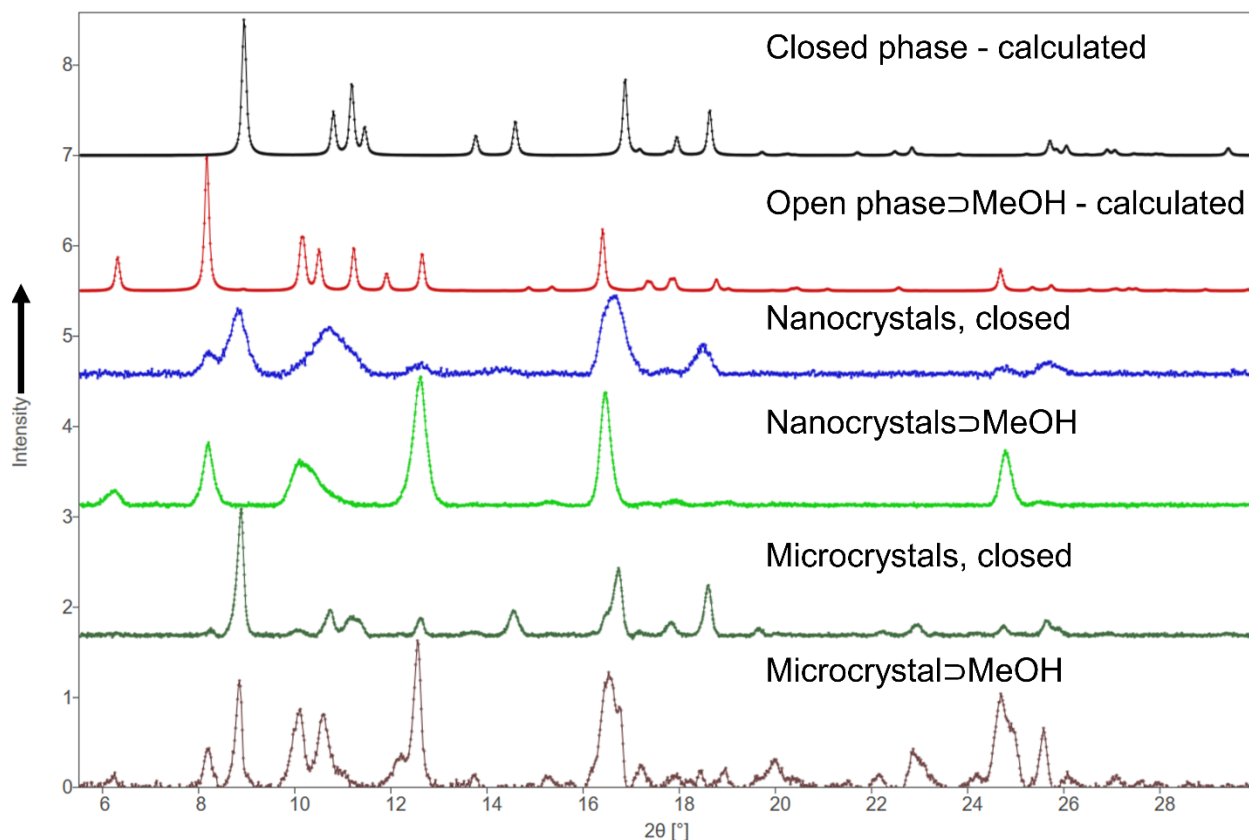


Figure S1. Comparison of $[\text{Cu}_2(\text{bdc})_2(\text{bpy})]_n$ PXRD patterns: calculated patterns from X-ray single crystal data (black, red), nanocrystals after heating at 200 °C for 1 hour (blue), as-synthesized nanocrystals via coordination modulation in methanol (light green), microcrystals after heating at 65 °C overnight (dark green), and methanol-filled microcrystals (brown).

The PXRD pattern of the crystals formed by solvothermal synthesis (Fig. S1, blue) is in line with the calculated and experimental patterns of the closed phase (Fig. S1, red). Powder patterns of the nanocrystals formed by coordination modulation (gray, maroon) are also consistent with previous data.¹ We note that PXRD patterns of $[\text{Cu}_2(\text{bdc})_2(\text{bpy})]_n$ may contain peaks corresponding to both the open and closed phases of the framework, where $2\theta = 6.3^\circ$ and 8.2° are characteristic of the open phase containing methanol as a guest molecule, while $2\theta = 8.9^\circ$ is only found in the predicted pattern for the closed, empty phase. For the sample synthesized solvothermally, the $2\theta = 8.9^\circ$ peak intensity is approximately two times larger than that at $2\theta =$

8.2°. Additionally, $2\theta = 6.3^\circ$ peak is present at a low intensity, indicating a possible mixture of closed and open phases of the framework. The open dried phase is a transient state which is known to be kinetically stabilized at the nanoscale.¹ PXRD analyses of the nanocrystals exhibits mixed phase patterns, although significant peak broadening at $2\theta = \sim 10\text{-}11.5^\circ$ is attributed to effects of crystal downsizing. Notably, as-synthesized nanocrystals of $[\text{Cu}_2(\text{bdc})_2(\text{bpy})]_n$ are predominantly in the open dried phase of the framework (Fig. S1, gray). After heating the sample at the shape-memory transition temperature (200 °C) for 1 hour, the $2\theta = 6.3^\circ$ peak corresponding to the open phase is diminished along with a concurrent increase and decrease of the $2\theta = 8.9^\circ$ and 8.2° peaks, respectively. The PXRD patterns reveal the efficacy of shape-memory transitions at the nanoscale.

3) Atomic Force Microscopy (AFM) imaging and nanoindentation measurements

Micro-sized $[\text{Cu}_2(\text{bdc})_2(\text{bpy})]_n$ crystals ranging from 2-20 μm were drop-casted from methanol onto a freshly cleaved atomically flat mica substrate (V-1 grade, SPI Supplies, Westchester, PA). Nano-sized crystalline samples were suspended in methanol (~ 800 mg in 1 mL), then drop-casted onto a freshly cleaved mica substrate and solvent was left to evaporate for 10 minutes. We expect that samples drop casted onto substrates are to be in the open phase due to pore interaction with the methanol solvent. All AFM studies were conducted using a Molecular Force Probe 3D AFM (Asylum Research, Santa Barbara, CA). For microcrystals, AFM images and nanoindentation measurements were collected at room temperature and ambient pressure using Si_3N_4 probes (Mikromasch, San Jose, CA, HQ:NSC36/Al BS) with a nominal spring constant of 1 N/m and a typical tip radius of 8 nm. A total of 82 and 24 force curves were collected on the microcrystals in the open and closed phases, respectively. For nano-sized samples, AFM images and nanoindentation measurements were collected at room temperature and ambient pressure using

Si₃N₄ probes coated with synthetic diamond (Mikromasch, San Jose, CA, HQ:NSC36/HARD/Al BS) with a nominal spring constant of 1 N/m and a typical tip radius of 25-35 nm. The actual tip radius of curvature was measured using Gwiddyion SPM tip size analysis across three different calibration images for an average radius of 30 nm.² Actual spring constants were determined using a built-in thermal noise method.³ A total of 227 and 30 force plots were collected on nanocrystals in the open and closed phases, respectively. Topographic images were collected using an intermittent contact mode (AC mode) or a contact mode at a typical scan rate of 1 Hz.

AFM nanoindentation experiments were performed by recording force versus vertical piezo displacement curves to determine Young's modulus values of individual micro- and nano-sized [Cu₂(bdc)₂(bpy)]_n single crystals. The Young's modulus was determined by fitting the loading force *versus* indentation depth approach data to the Johnson-Kendall-Roberts (JKR) elastic contact model.⁴ Here, the Young's modulus and Poisson's ratio of the AFM probe were assumed to be 865 GPa and 0.20, respectively. The Poisson's ratio of the [Cu₂(bdc)₂(bpy)]_n crystals was assumed to be 0.30.⁵ The JKR model was selected due to close overlap between the approach and retract contact region data, confirming purely elastic nanoindentation, and the presence of an adhesion force (ca. 6–20 nN) between the AFM tip and [Cu₂(bdc)₂(bpy)]_n samples. The acquisition of the force plots and corresponding data analysis were carried out as reported in our previous work.⁶⁻⁹ The applied mechanical during AFM nanoindentation based on the applied loading force per contact area calculations were typically 40-50 MPa for both micro- and nanocrystals. Nominal force values were between 10-40 nN depending on the material stiffness.

4) References

1. Sakata, Y.; Furukawa, S.; Kondo, M.; Hirai, K.; Horike, N.; Takashima, Y.; Uehara, H.; Louvain, N.; Meilikhov, M.; Tsuruoka, T.; Isoda, S.; Kosaka, W.; Sakata, O.; Kitagawa, S. *Science*. **2013**, *339*, 193-196.

2. Nečas, D.; Klapetek, P. *Cent. Eur. J. Phys.* **2012**, *10* (1), 181-188.
3. Hutter, J.L.; Bechhoefer, J. *Rev. Sci. Instrum.* **1993**, *64*, 1868.
4. Johnson, K.L.; Kendall, K.; Roberts, A.D. *Proc. Royal Soc. A.* **1971**, *324*, 301-313.
5. Henke, S.; Li, W.; Cheetham, A. K. *Chem. Sci.* **2014**, *5*, 2392-2397.
6. Rupasinghe, T.P.; Hutchins, K.M.; Bandaranayake, B.S.; Ghorai, S.; Karunatilake, C.; Bučar, D.K.; Swenson, D.C.; Arnold, M.A.; MacGillivray, L.R.; Tivanski, A.V. *J. Am. Chem. Soc.* **2015**, *137*, 12768-12771.
7. Hutchins, K.M.; Rupasinghe, T.P.; Oburn, S.M.; Ray, K.K.; Tivanski, A.V.; MacGillivray, L.R.; *CrystEngComm.* **2019**, *21*, 2049.
8. Karunatilaka, C.; Bučar, D.K.; Ditzler, L.R.; Friscic, T.; Swenson, D.C.; MacGillivray, L.R.; Tivanski, A.V. *Angew. Chem. Int. Ed.* **2011**, *50*, 8642-8646.
9. Tiba, A. A.; Tivanski, A. V.; MacGillivray, L. R. *Nano Lett.* **2019**, *19*, 6140-6143.